

controversial issue. For instance, although it is generally believed that the slow deocclusion of K^+ in the absence of ATP and occlusion of the cation via the direct route occur from sites exposed to the intracellular medium, there is no conclusive evidence in this respect (7). On the other hand, it has been observed that at least one of the two Rb^+ ions occluded via the direct route seems to be released to the extracellular medium (8).

The experiments presented in this paper were designed to investigate if the sites of the Na^+/K^+ -ATPase that are involved in the occlusion/deocclusion of K^+ through the direct route are exposed to the intracellular or the extracellular surface of the membrane. The rationale of the experiments lies on two propositions: (i) in the absence of ATP, deocclusion of K^+ and its congeners appear to be a sequential process where two ions are released according to a single file mechanism, both in the absence and in the presence of $Mg + Pi$, (8, 9) and (ii) in the presence of $Mg + Pi$, exchange of K^+ would take place through sites exposed to the extracellular surface of the membrane (6).

We hope that the present work will contribute to clarify the nature of the processes involved in the transport mechanism and to identify the ligands of the pump that determines the K^+ -binding sites to be exposed to one or the other surface of the membrane.

A preliminary report of part of the results in this work were presented at the 10th Conference on Na, K -ATPase and Related Cation Pumps, in 2002 (10).

MATERIALS AND METHODS

Na^+/K^+ -ATPase was a partially purified preparation from pig kidney according to the procedure of Jensen et al. (11). The specific activity of the preparation in optimal conditions (150 mM NaCl, 20 mM KCl, 3 mM ATP, 4 mM $MgCl_2$ and 25 mM imidazole-HCl, pH 7.4) measured at 37 °C ranged from 20 to 24 $\mu\text{mol Pi min}^{-1} (\text{mg protein})^{-1}$.

Reagents and Reaction Conditions. [^{86}Rb]RbCl ($^{86}\text{Rb}^+$) was obtained from Perkin-Elmer NEN Life Sciences (USA). All other reagents were of analytical grade. Experiments were performed at 25 °C in media containing 25 mM imidazole-HCl (pH 7.4 at 25 °C) and 0.25 mM EDTA. The concentrations of other components varied according to the experiments and are indicated in Results.

Measurement of Rubidium Occlusion. The amount of Rb^+ occluded was measured following the procedure described by Rossi et al. (4) Briefly, the reactions were performed either in a test tube or in a rapid-mixing apparatus (RMA) (SFM4 from Bio-Logic, France). To stop the reaction and isolate Rb^+ -bound enzyme from the free Rb^+ in the solution the reaction mixture was injected from the RMA into a quenching-and-washing chamber (QWC). In the moment of the injection, an ice-cold washing solution with 30 mM KCl and 20 mM imidazole-HCl (pH 7.4 at 0 °C) was flowing at a rate of 40 mL/s through a Millipore filter (0.8 μm) placed in the QWC. Occluded Rb^+ was considered equal to that retained by the enzyme after washing with at least 300 mL of the ice-cold washing solution, after subtracting the blank values. These were estimated from the amount of $^{86}\text{Rb}^+$ retained by the filters in the absence of enzyme and were usually much lower than 10% of the amount of occluded $^{86}\text{Rb}^+$.

The Time Course of Rb^+ Deocclusion. This was done measuring the amount of $^{86}\text{Rb}^+$ occluded as a function of time after diluting an enzyme suspension as explained in the figure legends. Dilution of $^{86}\text{Rb}^+$ in the enzyme suspension was at least 10-fold and the specific activity was either unchanged or decreased 400-fold as a maximum by adding unlabeled Rb^+ .

In order to obtain better estimations of the rate coefficients for $^{86}\text{Rb}^+$ release in the presence of $Mg + Pi$, where the reaction is faster, it was important to determine the amount of occluded Rb^+ at zero time independently of the value extrapolated from the time courses. Three different protocols were employed depending on the experimental setup: (a) an extrapolation at time = 0 from a similar time course where $Mg + Pi$ was absent, (b) an extrapolation at time = 0 from a similar time course where free Mg^{2+} was chelated with excess EDTA, or (c) measuring occluded Rb^+ after dilution in a medium where the concentration and specific activity of $^{86}\text{Rb}^+$ were kept unchanged with respect to that in the original enzyme suspension.

Double Incubation Sequence. The aim of this double incubation sequence was to obtain a suspension of the enzyme that holds one radioactive Rb^+ and one unlabeled Rb^+ in either position I or II (see scheme in Figure 2 below). This can be done in view of the great difference in the exchange rates between the two Rb^+ ions at high $[Rb^+]$. To locate $^{86}\text{Rb}^+$ in position I the enzyme was first equilibrated in media with 100 μM unlabeled Rb^+ and then suspended for a short time (88 ms or 48 s in media with or without $Mg + Pi$, respectively) in a solution containing 500 μM $^{86}\text{Rb}^+$. Conversely, to locate $^{86}\text{Rb}^+$ in position II, equilibration was achieved in media with 100 μM $^{86}\text{Rb}^+$ and the short incubation was carried out in media with 500 μM Rb^+ , accompanied by a 20-fold isotopic dilution.

Rb^+ Occluded in Equilibrium Conditions. Thirty $\mu\text{g/mL}$ of Na^+/K^+ -ATPase were incubated during 15 to 120 min in media containing different concentrations of $^{86}\text{Rb}^+$ and with or without 3 mM $MgCl_2$ and 8 mM Pi.

Data Analysis and Development of Theoretical Models. Equations were adjusted to the results by nonlinear regression using commercial programs, such as Excel and Sigma-Plot for Windows, the latter being able to provide not only the best fitting values of the parameters but also their standard errors. The goodness of fit of a given equation to the experimental results was evaluated by the corrected AIC criterion defined as

$$AIC_c = N \ln(SS/N) + 2PN/(N - P - 1)$$

where N is the number of data, P is the number of parameters plus one, and SS is the sum of weighted square residual errors (12). Unitary weights were considered in all cases and the best equation was chosen as that giving the lower value of AIC_c . The AIC criterion is based on the Information Theory, and selects an equation among several possible equations on the basis of its capacity to explain the results using a minimal number of parameters.

To fit numerical solutions of the kinetic models we employed a procedure based on the Gauss–Newton algorithm (13) developed by us for its use in Mathematica for Windows (14).

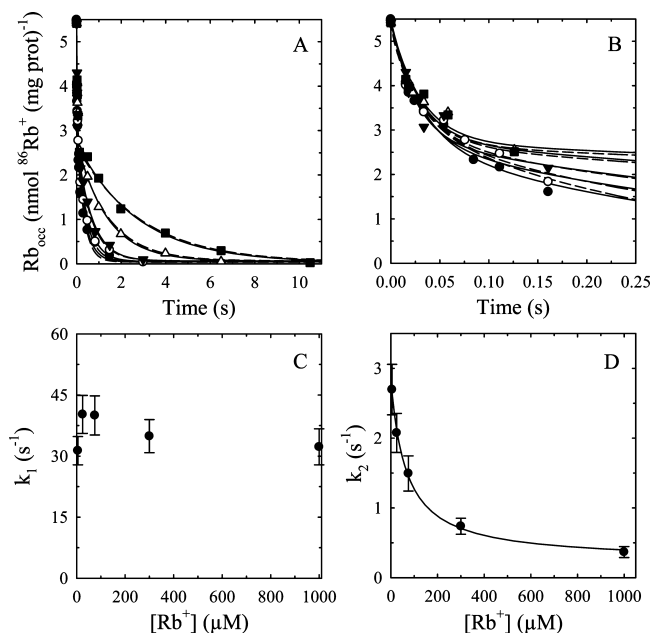


FIGURE 1: Release of occluded Rb⁺ in the presence of Mg + Pi at different concentrations of Rb⁺. Enzyme (600 μg/mL) was incubated in a medium containing 100 μM ⁸⁶Rb⁺ for 15–120 min to ensure equilibrium. One volume of this suspension was mixed with 19 volumes of a medium containing enough MgCl₂, inorganic orthophosphate (Pi), and RbCl to reach final concentrations of 3 mM MgCl₂, 8 mM Pi, and either 5 (●), 25 (○), 75 (▼), 300 (▽), or 1000 (■) μM Rb⁺ (panels A and B). Values of Rb_{occ} at time = 0 were obtained measuring occluded ⁸⁶Rb⁺ after dilution in a medium where the concentration and specific activity of ⁸⁶Rb⁺ were kept unchanged with respect to that in the original enzyme suspension. The time courses are shown in panels A and B, the latter being a detail of the first 250 ms of the reaction. The continuous lines are the plot of eq 1 that gave best fit to the experimental data. Dashed lines are the solution of the equations of model in Figure 7 for the best fitting values of the rate constants in Table 2. In panels C and D we show, respectively, the best fitting values of the parameters k_1 and k_2 (eq 2) as a function of [Rb⁺]. Vertical bars are ± 1 SE. Continuous line in panel D is the plot of eq 2 using the best fitting values of the parameters (see main text).

RESULTS

Rb⁺ Release in the Presence of Mg²⁺ and Pi. ATPase preparations were equilibrated in media with 100 μM ⁸⁶Rb⁺ and then the time course of Rb⁺ release was followed in media with 3 mM MgCl₂, 8 mM Pi, and from 5 to 1000 μM Rb⁺. Results in Figure 1 show that in all conditions the time courses could be described by the sum of two exponential functions of time plus a constant, positive term, that is

$$Rb_{occ} = A_1 e^{-k_1 t} + A_2 e^{-k_2 t} + A_{\infty} \quad (1)$$

The goodness of fit improved when $A_1 = A_2$. Panels C and D in Figure 1 also show the best fitting values of the rate coefficients, k_1 and k_2 , at different concentrations of Rb⁺. It can be seen that, as [Rb⁺] increases, the values of k_1 do not vary significantly, while those of k_2 decrease tending to a small, positive value, following eq 2:

$$k_2 = \frac{(k_{2,0} - k_{2,\infty}) K_1}{[Rb^+] + K_1} + k_{2,\infty} \quad (2)$$

where $k_{2,0}$ and $k_{2,\infty}$ are the values of k_2 when [Rb⁺] is equal to zero or tends to infinity, respectively, and K_1 is the Rb⁺

concentration at which the value of k_2 equals the average between $k_{2,0}$ and $k_{2,\infty}$. The best fitting values of these parameters (± 1 SE) were $k_{2,0} = 2.645 \pm 0.093 \text{ s}^{-1}$, $K_1 = 65 \pm 11 \text{ μM}$, and $k_{2,\infty} = 0.238 \pm 0.082 \text{ s}^{-1}$. These values of rate coefficients, which are much higher than those observed in the absence of Mg + Pi (see ref 5), agree very well with results obtained by Forbush (see Figure 4 in ref 8).

Results in Figure 1 can be explained if Rb⁺ occlusion occurred through a single-file mechanism, (5, 8, 9) a simplified version of which is shown in the scheme in Figure 2. Recent results on the crystal structure of the Na⁺/K⁺-ATPase with two Rb⁺ occluded give support to this scheme showing that the two ions share a common cavity (1). This would also explain the decrease of k_2 , since the increase of unlabeled [Rb⁺] (black circles in the scheme) in the reaction medium will decrease the probability to find the position I empty and therefore the rate of release of the ⁸⁶Rb⁺ (white circles) in position II. In other words, unlabeled Rb⁺ “blocks” the release of the ⁸⁶Rb⁺ occluded in position II, a result that is consistent with those obtained by Glynn et al., (9) and by Forbush (8). Additionally, the scheme predicts that the rate of release of ⁸⁶Rb⁺ from position I should not vary significantly with the concentration of Rb⁺, a fact that is reflected in the scarce variability of the values of k_1 with [Rb⁺] (Figure 1C). In view of these properties, it is easy to see why the scheme in Figure 2 also provides the rationale for a procedure to obtain occluded states with two Rb⁺ ions in which only one Rb⁺ is labeled (see Materials and Methods).

Sidedness of Rb⁺ Exchange via the Direct Route. In the scheme in Figure 2, where only the gate in position I can be open, the last Rb⁺ entering the enzyme should be the first to leave. In terms of experimental results, the release of the Rb⁺ closer to the open gate, that is, the last entering Rb⁺, will be much faster than for the Rb⁺ occluded in the deeper position. If addition of Mg + Pi changed the conditions so that the open gate were that closer to position II, now the first Rb⁺ to be released would be that which first entered the enzyme in the absence of Mg + Pi, and its rate of release will be fast.

To test these predictions we selectively replaced one of the two Rb⁺ ions with ⁸⁶Rb⁺ in the absence of Mg + Pi (the exchange time was 48 s) and then measured ⁸⁶Rb⁺ release in the presence of Mg + Pi. Results are shown in Figure 3A. When ⁸⁶Rb⁺ was in position II its release was slow whereas when ⁸⁶Rb⁺ was in position I, its release was fast. In both cases, if the scheme in Figure 2 held, the results indicate that release of Rb⁺ took place to the same surface of the membrane from which it was occluded.

Therefore, according to the currently accepted effects of Mg + Pi on E2(Rb₂), (6) exchange of Rb⁺ via the direct route should have occurred through the extracellular gate.

Using conditions estimated from the results in Figure 1, control experiments were performed on enzyme that was first equilibrated with Rb⁺, and Mg + Pi was added during the second step of the incubation sequence and present thereafter (panel B), or where Mg + Pi was absent both during the double incubation sequence and during measurement of ⁸⁶Rb⁺ release (panel C). For the experiment whose results are shown in panel B, the enzyme was allowed to exchange its outermost Rb⁺ for 88 ms through the extracellular access before deocclusion of ⁸⁶Rb⁺ was measured. The results are

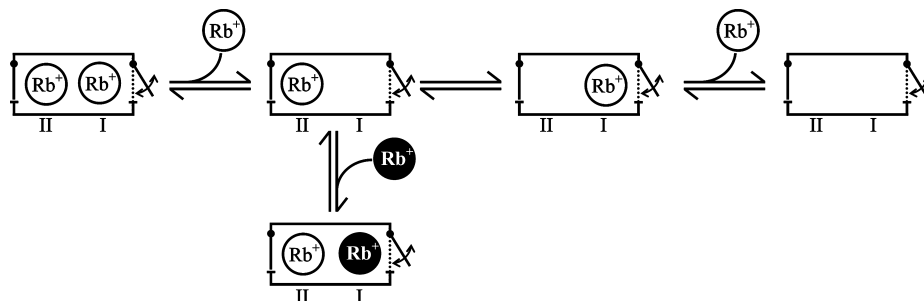


FIGURE 2: A scheme for occlusion and release of $^{86}\text{Rb}^+$ through the direct route showing the blockage by Rb^+ in the medium. The box represents the enzyme with two gates. The occlusion sites can be exposed to any of the surfaces of the membrane depending on which gate is open. During occlusion both gates are closed. We assume that, under the experimental conditions used in this work, the gate in position I is open much more frequently than the other so that almost all the exchange of Rb^+ will take place through this gate. The first Rb^+ to leave the enzyme will be that in position I. The release of the Rb^+ placed in position II requires position I to be empty. For this reason, in a medium with high Rb^+ concentration the rate of release of the ion in position II is very slow. A state containing one labeled and one unlabeled Rb^+ is represented in the bottom of the vertical branch.

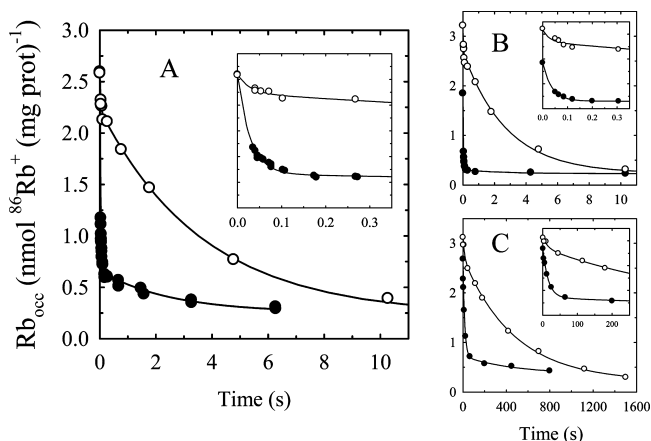


FIGURE 3: The time course of release of occluded $^{86}\text{Rb}^+$ in position I or II in the presence and in the absence of $\text{Mg} + \text{Pi}$. One volume of enzyme containing labeled Rb^+ was mixed with 9 volumes of a solution with unlabeled Rb^+ to obtain at least a 20-fold specific activity dilution and a final concentration of $1000 \mu\text{M} \text{Rb}^+$. The release of $^{86}\text{Rb}^+$ was measured in media with $3 \text{ mM} \text{Mg}^{2+}$ and $8 \text{ mM} \text{Pi}$ (panels A and B) or without Mg and Pi (panel C). The enzyme containing one labeled and one unlabeled Rb^+ was obtained after a double incubation sequence as explained under Materials and Methods either in the absence (panels A and C) or in the presence (panel B) of Mg and Pi . After the double incubation sequence, the majority of radioactive Rb^+ was placed either in position I (\bullet) or in position II (\circ). Values of Rb_{occ} at time = 0 were obtained as an extrapolation from a similar time course where either $\text{Mg} + \text{Pi}$ was absent (panel A) or free Mg^{2+} was chelated with excess EDTA (panel B). Insets are a detail of the first 0.35 s (panels A and B) or 250 s (panel C). The continuous lines are the plot of eq 1 for the best fitting values of its parameters.

very similar to those shown in panel A, confirming that exchange in the absence and in the presence of $\text{Mg} + \text{Pi}$ occurs through the same (extracellular) access. In the absence of $\text{Mg} + \text{Pi}$ both during the exchange phase and during $^{86}\text{Rb}^+$ release (panel C), the time courses agree qualitatively with the results observed in panel A and B except for the fact that the reactions are much slower.

The best fit of the curves in Figure 3 were achieved using the sum of two exponential functions of time (eq 1), in which the size of one phase is at least 82% that of the maximal change. Although most of the occluded $^{86}\text{Rb}^+$ will be predominantly located in one of the two positions after the double incubation sequence, it is difficult to prevent a minor fraction to occupy the other position, which explains the presence of a small second component (as predicted by the

Table 1: Best Fitting Values of the Parameters of eq 1 after Regression Analysis of the Results in Figure 3^a

panel in Figure 3	predominant form	$k_1 \text{ (s}^{-1}\text{)}$	$A_1 \text{ (\%)}$	$k_2 \text{ (s}^{-1}\text{)}$	$A_2 \text{ (\%)}$
A	(Rb)E2(^{86}Rb)	35.8 ± 1.5	83.26	0.64 ± 0.17	16.74
	(^{86}Rb)E2(Rb)	29.6 ± 6.8	15.78	0.266 ± 0.015	84.22
B	(Rb)E2(^{86}Rb)	30.1 ± 1.4	91.28	3.6 ± 1.5	8.72
	(^{86}Rb)E2(Rb)	35	17.64	0.363 ± 0.031	82.36
C	(Rb)E2(^{86}Rb)	0.0657 ± 0.0091	85.51	0.0030 ± 0.0041	14.49
	(^{86}Rb)E2(Rb)	0.041 ± 0.019	15.91	0.0020 ± 0.0002	84.09

^a A_1 and A_2 are expressed as the percentage of the maximal change, $A_1 + A_2$. The predominant form refers to the more abundant state containing one labeled and one unlabeled occluded Rb^+ after the double incubation sequence; occluded Rb^+ at the left of E2 is located in the deeper part of the pocket.

simulation of the model in ref 5). The best fitting values of the rate coefficients of eq 1 are shown in Table 1.

In media with $\text{Mg} + \text{Pi}$ (panels A and B), the rate coefficients of $^{86}\text{Rb}^+$ release from the major components show no significant differences when compared with those obtained from the complete curves in Figure 1. The same holds for the rate coefficients of $^{86}\text{Rb}^+$ release of the major components in media without $\text{Mg} + \text{Pi}$ (panel C) as compared with those we previously reported for their corresponding complete curves, (5) that is, $k_1 = 0.0754 \pm 0.0057 \text{ s}^{-1}$ and $k_2 = 0.0038 \pm 0.00034 \text{ s}^{-1}$. Notice that the rate coefficients of the minor phases were poorly estimated and their comparison is less reliable.

Blocking Effects of Rb^+ on the Slow Phase of $^{86}\text{Rb}^+$ Release from States with One Labeled and One Unlabeled Rb^+ in the Presence $\text{Mg} + \text{Pi}$. If the coefficients of the slow phase corresponded to the $^{86}\text{Rb}^+$ in position II then, the rate of release of occluded $^{86}\text{Rb}^+$ should decrease with Rb^+ concentration. To test this prediction we measured the release of occluded $^{86}\text{Rb}^+$ mainly located in position II in media with different concentrations of Rb^+ (Figure 4A,B).

It can be seen that when the concentration of Rb^+ in the deocclusion media increases, the rate of release of $^{86}\text{Rb}^+$ decreases. Each curve was fitted by eq 1 (continuous lines in Figure 4A,B). Because of the small size and high velocity of the fast component, which makes the estimation of its parameters difficult, the corresponding rate coefficient k_1 was fixed at the average value, 35 s^{-1} (Figure 1C). Inclusion of this restriction in the fitting procedure lowered the value of AIC_C .

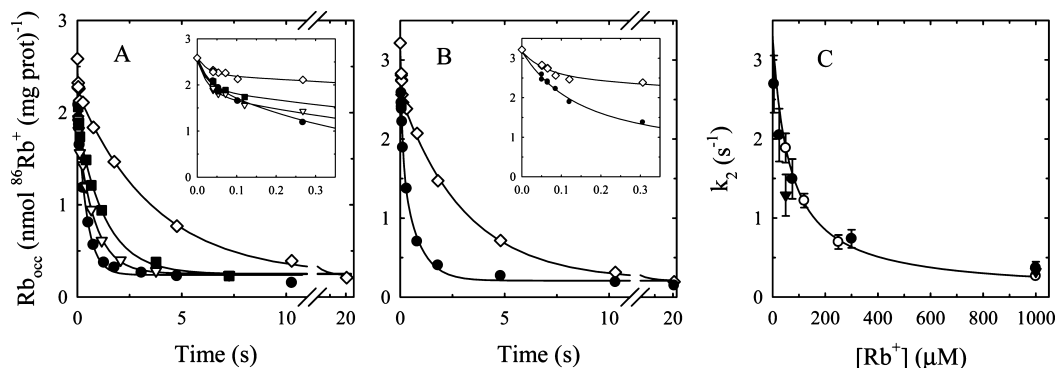


FIGURE 4: Time courses of $^{86}\text{Rb}^+$ release from position II at different $[\text{Rb}^+]$. Panels A and B show measurements of the amount of $^{86}\text{Rb}^+$ that remains after isotopic dilution in media with different concentrations of unlabeled Rb^+ , of an enzyme suspension containing the $^{86}\text{Rb}^+$ mostly in position II. This suspension was obtained either in the absence (panel A) or in the presence (panel B) of $\text{Mg} + \text{Pi}$ carrying out the double incubation sequence (see Materials and Methods). The concentration of Rb^+ in the reaction media were 50 (●), 100 (▽), 250 (■), and 1000 (◇) μM . Values of Rb_{occ} at time = 0 were obtained as an extrapolation from a similar time course where either $\text{Mg} + \text{Pi}$ was absent (panel A) or free Mg^{2+} was chelated with excess EDTA (panel B). Insets show a detail of the first 350 ms of the time courses. The continuous lines are plots of eq 1 for the best fitting values of its parameters. For the rest of the conditions and procedures see legend to Figure 3. Panel C shows the values of k_2 that were obtained fitting eq 1 to each experimental curve in panel A (○) and B (▼). Vertical bars are $\pm 1\text{SE}$. The continuous line is a plot of eq 2 using the best fitting values of its parameters shown in the main text. Values of k_2 for the experiments in Figure 1 (●) were superimposed.

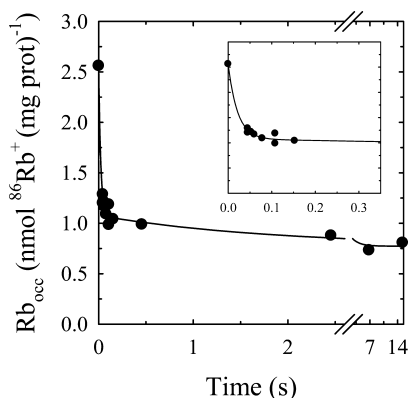


FIGURE 5: $^{86}\text{Rb}^+$ release after a very short preincubation with the cation. Enzyme (269 $\mu\text{g}/\text{mL}$) was preincubated during 360 ms with 200 μM $^{86}\text{Rb}^+$ and one volume of this reaction medium was mixed with 9 volumes of a solution with unlabeled Rb^+ and $\text{Mg} + \text{Pi}$ to reach final concentrations of 1000 μM Rb^+ , 3 mM MgCl_2 , and 8 mM Pi . The value of Rb_{occ} at time = 0 was obtained as an extrapolation from a similar time course where $\text{Mg} + \text{Pi}$ was absent. Inset shows a detail of the first 350 ms of the time course. The continuous line is a plot of eq 1 for the best fitting values of its parameters, which were $A_1 = 1.483 \pm 0.073$ nmol $^{86}\text{Rb}^+$ (mg protein) $^{-1}$, $k_1 = 46.5 \pm 6.7$ s^{-1} , $A_2 = 0.304 \pm 0.058$ nmol $^{86}\text{Rb}^+$ (mg protein) $^{-1}$, $k_2 = 0.54 \pm 0.38$ s^{-1} , $A_\infty = 0.773 \pm 0.049$ nmol $^{86}\text{Rb}^+$ (mg protein) $^{-1}$.

Figure 4C shows the best fitting values of k_2 obtained from the curves of Figure 4A,B as a function of $[\text{Rb}^+]$. These values of k_2 , like those in Figure 1D, were better fitted by eq 2. The best fitting values of $k_{2,0}$, $k_{2,\infty}$, and K_1 obtained (3.44 ± 0.49 s^{-1} , 0.076 ± 0.022 s^{-1} , and 60 ± 15 μM , respectively) are not substantially different from those found from the values of k_2 in Figure 1D. This is also reflected by the superimposition of the points in panel C and indicates that the results are consistent with the model in Figure 2.

Occlusion of Rb^+ in Enzyme That Was Not Previously in Contact with the Cation. The experiments performed up to now started with the enzyme in media with Rb^+ , where the $E2$ conformation prevails. Under these conditions, exchange seems to take place through sites exposed to the extracellular surface of the membrane. It is generally assumed that the $E1$ conformation of the enzyme exposes its sites for Rb^+ to

the intracellular surface of the membrane (15). According to Fedosova and Esmann, (16) judging by its affinity for ADP at 25 mM imidazole at pH 7.4 and with no additional cations, the Na^+/K^+ -ATPase would be mostly in the $E1$ conformation. On this basis, enzyme suspended in a Rb^+ -free medium was incubated with $^{86}\text{Rb}^+$ during 360 ms and then the time course of $^{86}\text{Rb}^+$ release was measured in a medium with $\text{Mg} + \text{Pi}$ and 1 mM Rb^+ . Results obtained from control experiments (not shown) indicated that, in agreement with our previous work, (5) a time of 360 ms was long enough to fill more than 94% of the sites in position I and short enough to avoid a significant occupancy of the sites in position II (less than 5%). Results in Figure 5 show that about 60% of the initial amount of $^{86}\text{Rb}^+$ is rapidly released, while a significant fraction remains occluded. Results were adequately described with eq 1. If the best fitting value of A_∞ (see legend to Figure 5) were the true equilibrium value of the reaction, the size of the rapid phase would represent about 83% of the maximal change, a value that could agree with a model where Rb^+ is released to the same (the extracellular) surface of the membrane from which it was occluded. However, calculations based on the volume and isotopic dilutions indicate that the expected value for A_∞ was about 0.12 nmol $^{86}\text{Rb}^+$ (mg protein) $^{-1}$, which is more than 6-fold lower than the best fitting value obtained. This would imply that equilibrium was not reached yet and that the system is undergoing slower phases of the reaction, thus decreasing the true proportion of the fast phase. This might mean that either: (i) the enzyme starts from the $E1$ conformation, with both sites being similarly accessible from the intracellular face of the membrane, and an immediate transition to the $E2$ conformation occurs after the binding of one Rb^+ , or (ii) the enzyme starts from the $E2$ conformation, with only one of the two sites being accessible from the extracellular surface of the membrane and, after occupancy of this site with Rb^+ , the probabilities for the cation either to be released back to the solution or to jump to the deeper, empty site are comparable. In both cases, only about 50% of the release of Rb^+ would be rapid. The experiment in Figure 5 does not allow one to decide between these two possibilities or a

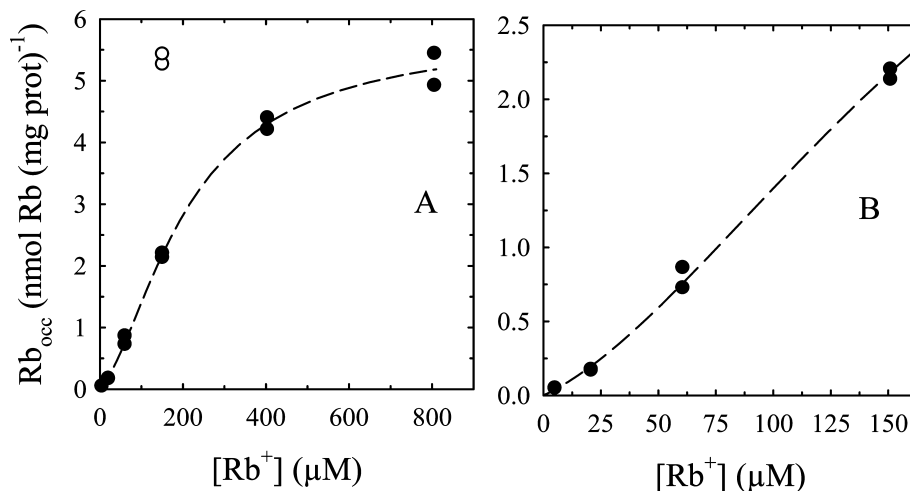


FIGURE 6: The equilibrium distribution between free and occluded Rb^+ in media with Mg + Pi. Rb_{occ} was measured after a 15 min incubation in media containing different concentrations of Rb^+ , 3 mM MgCl_2 , and 8 mM Pi (●). The open circles show the amount of Rb^+ occluded in media without Mg + Pi and 150 μM Rb^+ . The continuous line is the plot of the solution of the model in Figure 7 for the best fitting values of the parameters in Table 2. Panel B shows a detail of the values of Rb_{occ} up to 150 μM Rb^+ .

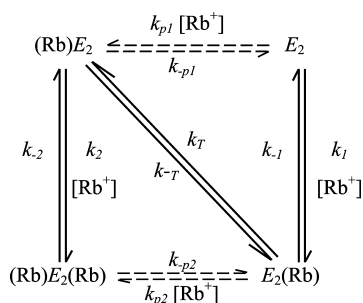


FIGURE 7: A scheme of the leaky single file model for Rb^+ occlusion in the presence of Mg + Pi. The Rb^+ shown in parentheses is occluded Rb^+ ; the occluded Rb^+ shown at the left of E_2 is located in the deeper part of the pocket. The presence of states with bound (but not occluded) Rb^+ were disregarded (see main text). The arrows drawn with continuous lines represent the pathways through which most of the reaction takes place, whereas the arrows drawn with dashed lines represent pathways that explain the very slow loss of occluded Rb^+ that persists when $[\text{Rb}^+]$ in the media tends to infinity.

combination of them, starting for instance with part of the enzyme in the E_1 and part in the E_2 conformation.

The Equilibrium Distribution between Free and Occluded Rb^+ in Media with Mg + Pi. We measured the amount of occluded Rb^+ in equilibrium conditions in media containing the same concentration of Mg + Pi used in the previous experiments of this work and different concentrations of Rb^+ (Figure 6). The occluded Rb^+ rose along a saturable, sigmoid function of $[\text{Rb}^+]$ with $K_{0.5} = 210 \pm 32 \mu\text{M}$. The amount of Rb^+ occluded when $[\text{Rb}^+]$ tends to infinity ($5.84 \pm 0.68 \text{ nmol Rb}^+ (\text{mg protein})^{-1}$) was not significantly different from that obtained in the absence of Mg + Pi (open circles in Figure 6A), indicating that the effect of Mg + Pi on Rb^+ occlusion can be reverted increasing the Rb^+ concentration. The slope of the curve at Rb^+ concentration tending to zero is larger than zero (see Figure 6B), suggesting either that a single Rb^+ could be occluded under these conditions (17) or that the concentrations of Mg^{2+} and Pi were not sufficiently high to saturate their effects on the enzyme.

A Model for Rb^+ Occlusion in the Na^+/K^+ -ATPase in the Presence of Mg + Pi. The model in Figure 7 allowed us to predict quantitatively both the rates of release of Rb^+ and

Table 2: The Best Fitting Values of the Rate Constants of the Model in Figure 7^a

	value \pm S. E.	units
k_1	0.575 ± 0.014	$\text{s}^{-1} \mu\text{M}^{-1}$
k_{-1}	459 ± 20	s^{-1}
k_T	0.90 ± 0.59	s^{-1}
k_{-T}	0.90 ± 0.59	s^{-1}
k_2	0.575 ± 0.014	$\text{s}^{-1} \mu\text{M}^{-1}$
k_{-2}	31.51 ± 0.94	s^{-1}
k_{p1}	0.00326 ± 0.00038	$\text{s}^{-1} \mu\text{M}^{-1}$
k_{-p1}	2.600 ± 0.031	s^{-1}
k_{p2}	0.00326 ± 0.00038	$\text{s}^{-1} \mu\text{M}^{-1}$
k_{-p2}	0.178 ± 0.032	s^{-1}
K_1	798 ± 65	μM
K_2	54.8 ± 2.5	μM

^a The value of total enzyme (± 1 SE) obtained from the fitting was $2.919 \pm 0.068 \text{ nmol (mg protein)}^{-1}$. The values of K_1 and K_2 were calculated as k_{-1}/k_1 and k_{-2}/k_2 , respectively.

the equilibrium amounts of occluded Rb^+ at different concentrations of the cation and in the presence of Mg + Pi. We used the model in Figure 7 to find the best fitting values of the parameters that describe the system. States with bound (but not occluded) Rb^+ were disregarded because they are probably only present in negligibly low concentrations. Note that the model in Figure 7 includes two pathways for a slow Rb^+ release which prevents total blockage on the occluded cation by Rb^+ in the reaction medium.

During the fitting procedure we applied the following constraints:

(a) the rate constant of Rb^+ occlusion for a given site was considered independent of the occupancy of the other site, that is:

$$k_1 = k_2 \quad (3)$$

and

$$k_{p1} = k_{p2} \quad (4)$$

(b) Rb^+ jumps with equal probability from position I to II and vice versa, that is

$$k_T = k_{-T} \quad (5)$$

Application of restrictions (a) and (b) improved the goodness of fit as judged by the decrease in the value of AIC_C (see Materials and Methods).

Additional restrictions on the values of the rate constants arose from the equivalence between the different pathways connecting the same initial and final states, that is

$$k_{-p1} = (k_{p1}k_{-1}k_{-T}) / (k_1k_T) \quad (6)$$

and

$$k_{p2} = (k_{-p2}k_2k_T) / (k_{-2}k_{-T}) \quad (7)$$

Table 2 shows the best fitting values of the rate constants of the model in Figure 7 and the calculated values of equilibrium dissociation constants for Rb⁺ (K_1 and K_2). Note that the value of K_2 is in good agreement with that of K_1 for the results of the rate coefficient k_2 as a function of [Rb⁺] (Figures 1D and 4C) as it would be expected if the Rb⁺ that produces the blocking effect becomes itself occluded (8). It is clear that the agreement between experimental results and those predicted by the model in Figure 7 (dashed lines in Figures 1 and 6) is excellent. In view of this and of its simplicity compared to possible alternative models we adopted the model in Figure 7 as the best explanation of the experimental results.

DISCUSSION

This paper provides evidence that occlusion and deocclusion of Rb⁺ from the $E2(Rb_2)$ state of the Na⁺/K⁺-ATPase take place through the same access that participates in the presence of Mg + Pi. Taking for granted that Mg + Pi promotes the exchange through an extracellular access, exchange of Rb⁺ between $E2(Rb_2)$ and the reaction medium via the direct route must occur when the transport sites are exposed to the extracellular surface of the membrane. We have to point out however that results presented in this paper do not allow one to determine whether occlusion of Rb⁺ in enzyme that was not previously in contact with the cation takes place from the cytoplasmic or from the extracellular surface of the membrane.

In their review of the role of occlusion in cation transport, Glynn and Karlsh (15) raised the question whether “the two main routes of occlusion of K⁺, coupled back-to-back, can provide a pathway capable of transporting the cation through the pump.” On the basis of the results in this paper, if the process occurs in the absence of ATP we would be inclined for a negative answer. The question posed by Glynn and Karlsh relies on former results by Karlsh and Pick (18) who found that only K⁺ ions with access to the intracellular surface can convert the enzyme to its $E2$ conformation. However, Karlsh and Stein (7) proposed later the possibility of Rb⁺ exchange directly from $E2(Rb_2)$, without a previous transition to $E1Rb_2$, saying that “the occluded form $E2(Rb_2)$ can undergo a transition to the form $E2Rb_2$ which is in equilibrium with the form $E2$ and Rb ions at the extracellular face of the pump.” Our results provide evidence for this proposal and answer questions raised by Forbush (8) on the sidedness of deocclusion via the direct route. Additionally, the present paper provides empirical support to observations by Jørgensen et al. (19) based on the crystal structure of the sarcoplasmic reticulum Ca²⁺-ATPase.

If the spontaneous exchange of Rb⁺ occurs through an extracellular access, it is worth asking about the meaning of the small leak of Rb⁺ observed under blocking concentrations of Rb⁺ in the reaction media. It could be that leakage occurs in the same direction as the main deocclusion flow, signifying that there is a breach between the deeper position and the occupied blocking site, so that the sequential nature of the process would not be strictly obligatory. Alternatively, the small leakage could be reflecting the fact that the enzyme is capable of opening to the opposite, cytoplasmic surface (likely in the $E1$ conformation), with very low frequency and for very short periods of time.

In view of our results, it remains an open question whether occlusion and deocclusion via the direct route participate in any significant degree in the transport of K⁺ during the ATPase activity. One could posit, for instance, that after dephosphorylation of $E2P(K_2)$, the slow release of K⁺ from those units of $E2(K_2)$ that are not combined with ATP occurs to the extracellular medium. If this were the case, these units would not be transporting K⁺ to the cytoplasm except perhaps in a fraction represented by the small leakage mentioned above, provided that this were accompanied by a transition to the $E1$ conformation of the dephosphoenzyme.

REFERENCES

- Morth, J. P., Pedersen, B. P., Toustrup-Jensen, M. S., Sørensen, T. L., Petersen, J., Andersen, J. P., Vilsen, B., and Nissen, P. (2007) Crystal structure of the sodium-potassium pump. *Nature* 450, 1043–1049.
- Beaugé, L. A., and Glynn, I. M. (1979) Occlusion of K ions in the unphosphorylated sodium pump. *Nature* 280, 510–512.
- Forbush, B., III (1984) An apparatus for rapid kinetic analysis of isotopic efflux from membrane vesicles and of ligand dissociation from membrane proteins. *Anal. Biochem.* 140, 495–505.
- Rossi, R. C., Kaufman, S. B., González-Lebrero, R. M., Nørby, J. G., and Garrahan, P. J. (1999) An attachment for nondestructive, fast quenching of samples in rapid-mixing experiments. *Anal. Biochem.* 270, 276–285.
- González-Lebrero, R. M., Kaufman, S. B., Montes, M. R., Nørby, J. G., Garrahan, P. J., and Rossi, R. C. (2002) The occlusion of Rb⁺ in the Na⁺/K⁺-ATPase. I. The identity of occluded states formed by the physiological or the direct routes: occlusion/deocclusion kinetics through the direct route. *J. Biol. Chem.* 277, 5910–5921.
- Forbush, B., III (1988) Overview: occluded ions and Na, K-ATPase, in *The Na⁺, K⁺-Pump. Part A, Molecular Aspects* (Skou, J. C., Nørby, J. G., Maunsbach, A. B., and Esmann M., Eds.) pp 229–248, Alan Liss, Inc., New York.
- Karlsh, S. J. D., and Stein, W. D. (1982) Passive rubidium fluxes mediated by Na-K-ATPase reconstituted into phospholipid vesicles when ATP- and phosphate-free. *J. Physiol.* 328, 295–316.
- Forbush, B., III (1987) Rapid release of ⁴²K or ⁸⁶Rb from two distinct transport sites on the Na,K-pump in the presence of Pi or vanadate. *J. Biol. Chem.* 262, 11116–11127.
- Glynn, I. M., Howland, J. L., and Richards, D. E. (1985) Evidence for the ordered release of rubidium ions occluded within the Na,K-ATPase of mammalian kidney. *J. Physiol.* 368, 453–469.
- González-Lebrero, R. M., Kaufman, S. B., Garrahan, P. J., and Rossi, R. C. (2003) The sidedness of the direct route of occlusion of K⁺ in the Na⁺/K⁺-ATPase. *Ann. N.Y. Acad. Sci.* 986, 301–303.
- Jensen, J., Nørby, J. G., and Ottolenghi, P. (1984) Binding of sodium and potassium to the sodium pump of pig kidney evaluated from nucleotide-binding behaviour. *J. Physiol. (London)* 346, 219–241.
- Burnham, K. P., and Anderson, D., R. (2002) *Model Selection and Multimodel Inference*, 2nd ed., pp 60–85, Springer, New York.
- Fraser, R. D. B., and Suzuki, E. (1973) The use of least squares in data analysis, in *Physical Principles and Techniques of Protein Chemistry: Part C* (Leach, S. J., Ed.) pp 301–355, Academic Press, New York.

14. González-Lebrero, R. M. (2001) *Caracterización cinética del fenómeno de oclusión de K^+ en la Na^+/K^+ -ATPasa*, Ph.D. thesis, University of Buenos Aires.
15. Glynn, I. M., and Karlish, S. J. D. (1990) Occluded cations in active transport. *Annu. Rev. Biochem.* 59, 171–205.
16. Fedosova, N. U., and Esmann, M. (2004) Nucleotide-binding kinetics of Na,K-ATPase: cation dependence. *Biochemistry* 43, 4212–4218.
17. González-Lebrero, R. M., Kaufman, S. B., Garrahan, P. J., and Rossi, R. C. (2002) The occlusion of Rb^+ in the Na^+/K^+ -ATPase. II. The effects of Rb^+ , Na^+ , Mg^{2+} or ATP on the equilibrium between free and occluded Rb^+ . *J. Biol. Chem.* 277, 5922–5928.
18. Karlish, S. J., and Pick, U. (1981) Sidedness of the effects of sodium and potassium ions on the conformational state of the sodium-potassium pump. *J. Physiol.* 312, 505–529.
19. Jørgensen, P. L., Håkansson, K. O., and Karlish, S. J. (2003) Structure and mechanism of Na,K-ATPase: functional sites and their interactions. *Annu. Rev. Physiol.* 65, 817–849.

BI800270K